ELSEVIER

Applied Surface Science 152 (1999) 99–106

applied surface science

www.elsevier.nl/locate/apsusc

Formation of self-assembled $Si_{1-x}Ge_x$ islands using reduced pressure chemical vapor deposition and subsequent thermal annealing of thin germanium-rich films

Rashid Bashir [a,*], Abul E. Kabir [b,1], Kuo-Jen Chao [c]

[a] *School of Electrical and Computer Engineering, Purdue University, West Lafayette, IN, USA*
[b] *Process Technology Development Group, National Semiconductor, Santa Clara, CA, USA*
[c] *Charles Evans and Associates, Sunnyvale, CA, USA*

Received 20 April 1999; accepted 22 June 1999

Abstract

In this study, we report on the initial experimental results of formation of self-assembled $Si_{1-x}Ge_x$ islands by the selective chemical vapor deposition of highly strained $Si_{1-x}Ge_x$ thin films (with $x \sim 0.4$) on patterned silicon wafers and the subsequent annealing of these thin films. Unlike previous studies, islands are formed during the thermal annealing of these thin films after the growth of the smooth continuous selectively grown thin films and not by direct growth of the islands. 50–160 Å $Si_{0.6}Ge_{0.4}$ films are selectively grown on silicon wafers with an oxide pattern using chemical vapor deposition from germane, silane and HCl at 650°C and 40 Torr. In situ annealing of the films at 650–750°C at 20–40 Torr for 6–25 min resulted in the formation of the islands. The size and distribution of the islands was found to be a function of the annealing conditions and an ordered pattern can be achieved with specific annealing conditions.

Keywords: $Si_{1-x}Ge_x$; Chemical vapor deposition; Thin germanium-rich films

1. Introduction

There have been numerous publications in the recent years that deal with the self-assembly of semiconductor islands on a crystalline substrate for the formation of quantum optical and electronic devices. The concept was initially demonstrated on III–V and II–VI family of semiconductor materials. A lattice mismatch material can be grown as a thin strained 2-D film on a substrate. Due to the strain energy from the lattice mismatch, after a certain thickness the growth proceeds by the 3-D Stranski–Krastanow (SK) mode in which the material will form small islands of random size and distribution. The main goal of the efforts in this area is to form ensembles of identical quantum size systems. For example, three-dimensional InAs [1–3] and InSb, GaSb, and AlSb [4] nanometer-scale dots have also been grown on GaAs. Work has also been reported to control the nucleation sites of the islands. For example, by depositing a GaAs nucleation site con-

* Corresponding author. Tel.: +1-765-496-6229; fax: +1-765-494-6441

[1] Present address: Linear Technology.

0169-4332/99/$ - see front matter
PII: S0169-4332(99)00306-2

trol layer, InAs can be grown on InP substrates with some regularity [5].

The SK growth technique has also been applied to silicon-based heterostructures, and pure Ge islands have been grown on silicon substrates [6–9]. These islands were grown using chemical vapor deposition from germane at 10 T to atmospheric pressure in a commercially available reactor through a modified Stranski–Krastanow (SK) growth process [7]. The same authors also show that preferential formation of Ge islands takes place at the edges of selective silicon region facet [8]. In a later study, it was also shown that once the islands are formed, subsequent annealing changes the shape and size of the islands as a function of annealing time [9]. Atoms can detach from one island and diffuse to other larger islands as function of thermal conditions, a phenomenon known as Ostwald ripening [7,10,11]. Very recently, the positioning of single-crystal Ge islands by Si mesas formed by nano-imprinting and etching has also demonstrated in an effort to achieve an ordered array of device islands [12]. The formation of these islands on a silicon substrate is especially attractive since this would allow possible integration of these quantum devices with existing silicon devices to form novel device structures. The silicon–germanium ($Si_{1-x}Ge_x$) material system is very attractive since it can be directly grown on silicon substrates. The possibility of integrating self-assembled nano-structures with silicon technology for electronic and optical applications provide great potential and promise to extend the silicon technology roadmaps.

In this letter, we report on the formation of ordered self-assembled $Si_{1-x}Ge_x$ islands by the selective CVD of very thin (< 160 Å) highly strained assembled $Si_{1-x}Ge_x$ ($x = 0.4$) films on patterned silicon wafers and the subsequent annealing of these thin films. Unlike previous studies, islands are formed during the thermal annealing of these thin films after the growth of the smooth continuous selectively grown thin film and not by direct growth of the islands.

2. Experimental details

A 3500 Å thermal oxide was formed using LOCOS (local oxidation of silicon) on 8″ silicon wafers. Various regions were defined on the wafers with an overall exposed area of about 15%. Thin $Si_{0.6}Ge_{0.4}$ films are selectively grown on the silicon wafers using a commercially available epitaxial system (ASM) in reduced pressure chemical vapor deposition conditions. A high temperature (950°C) H_2 bake for 10 min at 30 T was used to remove any native oxide prior to the growth. The films were then selectively deposited directly on the silicon exposed area at 40 T and 650°C. GeH_4 and $Si_2H_2Cl_2$ were used as the source gases and HCl was used to enhance selectivity over the oxide. The HCl to DCS ratio was 100 sccm/75 sccm. The wafers were inspected and no sign of defects or dislocations were observed. The growth was perfectly selective and no nucleation occurred over the oxide regions. Three specific regions were analyzed on the wafer. Region A consisted of a large square opening in the oxide, which was 50 μm on a side. Region B was the same overall size as region A but had 2 μm × 2 μm oxide islands with 1μm silicon open spaces between the oxide islands distributed evenly in the large overall square. Region C consisted of rectangular openings in the oxide, which were 3 μm wide and 50 μm long. After the growth, the wafers were brought out to atmosphere and analyzed using top-view scanning electron microscope and cross-sectional transmission electron microscopy.

3. Island characterization and discussion

Scanning electron microscope was used to inspect the as-grown films. Results showed a smooth film surface in the selective growth regions. Fig. 1 shows a high-resolution cross-sectional transmission electron microscopy through the region A depicting a film growth of about 55 Å. The picture does not show any defects or dislocation even though the film is most likely in a metastable regime. A similar TEM was also performed in region C along the narrow 2 μm width and the results showed a film growth of about 160 Å. Hence, there were loading effects present due to non-optimized growth conditions.

After the growth, the temperature was ramped up to 750°C and a wafer (#2) was in situ annealed in H_2 at 40 Torr for 6 min. Subsequent inspection of the films demonstrated the formation of islands in

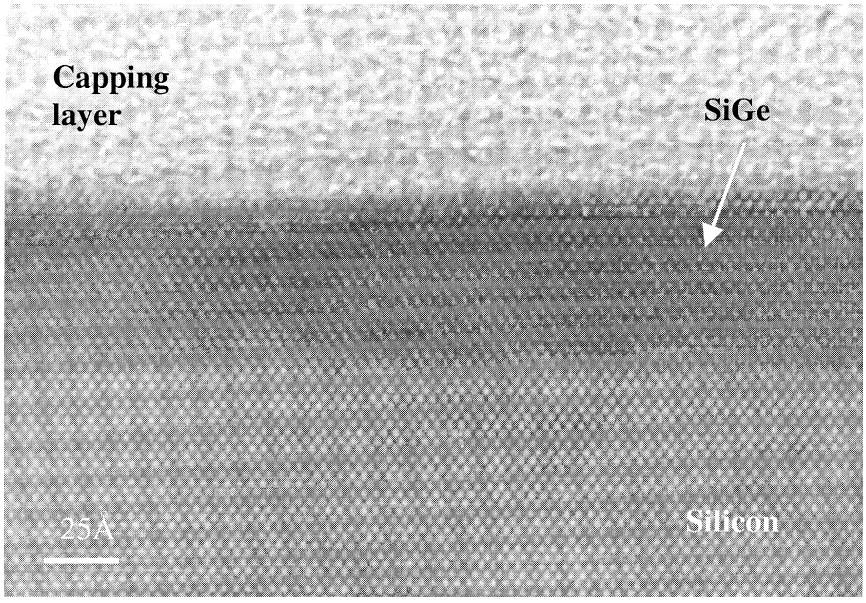

Fig. 1. Cross-sectional high-resolution TEM of the as-grown selective SiGe film in region A of wafer 1 (No annealing). The TEM does not show any defects or indications of relaxation.

the regions where the selective growth had taken place. Figs. 2 and 3 show an angled scanning electron microscope image of the island formed in regions A and B, respectively. The islands are larger

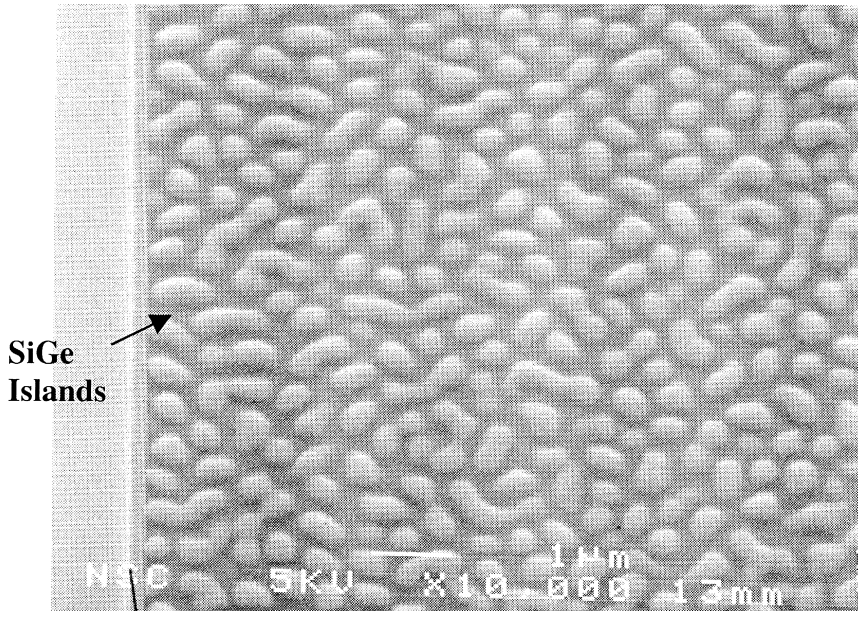

Fig. 2. Angled scanning electron microscope picture region A of wafer 2 after the thermal annealing (subsequent to the growth). Anneal was performed at 750°C for 6 min at 40 Torr in hydrogen.

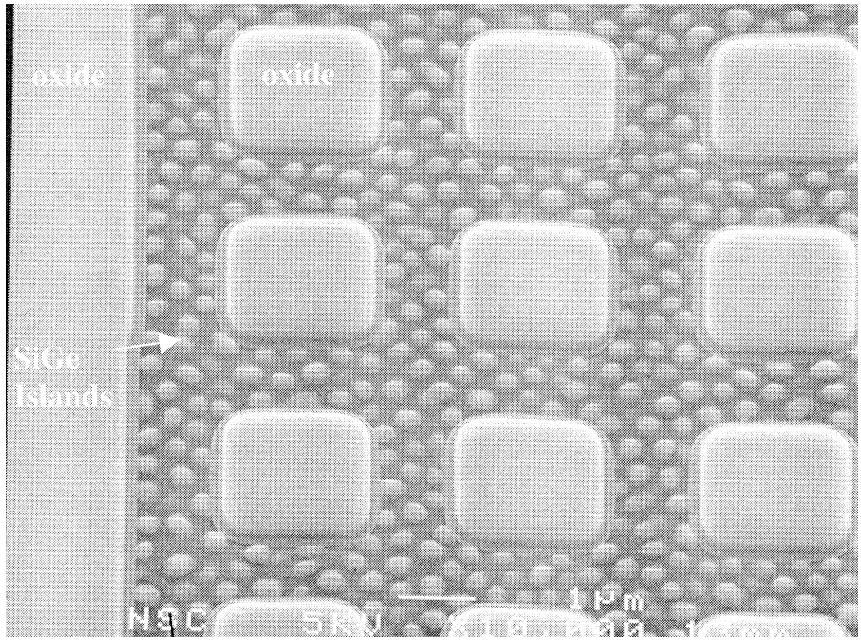

Fig. 3. Angled scanning electron microscope picture of region B of wafer 2 after the thermal annealing subsequent to the growth. Anneal was performed at 750°C for 6 min at 40 Torr in hydrogen. Islands are formed in the regions between the oxide where the film was initially grown selectively.

than the previously reported dots formed by SK growth of Ge on silicon substrates which were 20 to 75 nm wide [6,7]. The shape and distribution of the islands is different in the three regions could be due to variation in the film thickness (due to loading effects) or due to differences in the strain conditions owing to changes in exposed area. Separate experiments will need to be performed to separate and study these effects in more detail. Region B shows the most uniform and isolated regions when compared to the other two regions. The islands were studied using an atomic force microscope (Digital Instruments Nanoscope III Dimension 5000). The RMS roughness of a 10 μm $\times$ 10 μm area in region A of wafer # 2 (as shown in Fig. 2) was 23.6 nm. The island density was found to be about 3.2 μm^{-2}. From the roughness scans, the maximum height of the islands was found to be 102.5 nm also confirmed by a cross-sectional scan. Similarly, the RMS roughness of islands in between the oxide in Fig. 3 (region B) was found to be 20.7 nm, however, the island density was increased to about 6 μm^{-2} clearly indicating a reduction in size. From the roughness scans, the maximum height of the islands was found to be 127 nm.

Grain size analysis software from Digital Instruments was also used to determine the size distribution of the islands and was found to vary with the exposed silicon area. In the 10 μm $\times$ 10 μm area in region A of wafer #2, the mean grain size was found to be 1.29×10^5 nm^2 ($\sim$ 359 nm diameter assuming a circular shape) with a standard deviation of 6.62×10^4 nm^2 ($\sim$ 257 nm). The histogram of the island size in region A is shown in Fig. 4. As can be seen from the pictures in Fig. 2, and numerically demonstrated by the grain size analysis, there is a large variation in the island size. Specially, there are a few very large, oblong islands which increase the standard deviation. It is of course desirable to have the island size as uniform as possible.

Between the oxide patterns in region B, the mean grain size of the island was found to be 4.83×10^4 nm^2 ($\sim$ 245 nm diameter assuming a circular shape) with a std. deviation of 1.67×10^4 nm^2 ($\sim$ 139 nm). The histogram of the island size in region B is shown in Fig. 5. The island size and the standard

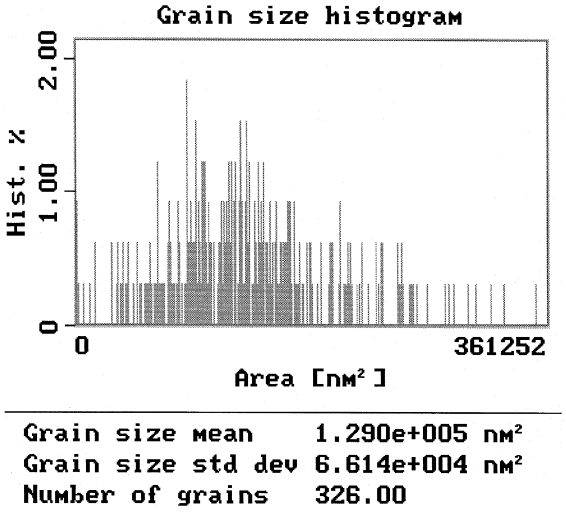

Fig. 4. Histogram of device island size from grain analysis of region A.

deviation has reduced when compared to the islands in region A. From the scanning electron microscope image of Fig. 3, the island size appears to be visually more uniform than the numerical values indicate. This could be attributed to the fact that while performing the graphical grain analysis, the oxide regions had to be removed from the analysis and could have resulted in partial removal of some of the islands close to the edges of the oxide. Hence, artificial small size islands might be included in the numerical grain size analysis. This observation can also be confirmed by the fact that the histogram in Fig. 5 is skewed towards the left (smaller grain size).

Fig. 6 shows a scanning electron microscope image of the region C. Even though this region is on the same wafer as the regions described above, the islands size and distribution is clearly very different in that the islands are oblong and connected to each other. Certainly this is not a condition to be desired for electronic and opto-electronic device applications. It should also be pointed out again that the initial film thickness in the small islands was found to be about 160 Å from TEM analysis and hence this variation in island size and morphology could be attributed to the higher starting film thickness. It can be conjectured that since there are more starting atoms available in this case and the Ostwald ripening, i.e., the migration of atoms towards island formation, was still progressing and a longer anneal could have made the island size smaller and more uniform. Cross-sectional TEM was also performed through region C and a representative image is shown in Fig. 7. The previously smooth film has clearly coalesced into islands. Grain size analysis was not performed on this region and only transmission electron microscope image is shown since the islands are almost all connected and are not isolated as grains.

It was also found that if the wafers were exposed to atmospheric ambient in air right after the growth, subsequent annealing of the films at 750°C at 40 T for 6 min in hydrogen did not result in the island formation. The passivation of the film by native oxide seems to make the surface more stable and increases the thermal energy required for the film to be relaxed. This particular phenomenon has also been observed by previous authors [6].

Different anneal conditions were explored to help make the islands more uniform and to help understand the underlying physical phenomenon. Another sample (wafer #3) was grown as described in Section 2 but the temperature of the in-situ anneal was reduced to 650°C for 25 min in hydrogen at 40 T. The film barely relaxed, i.e., visual scanning electron micrograph pictures revealed no island formation. AFM analysis showed an RMS roughness of only

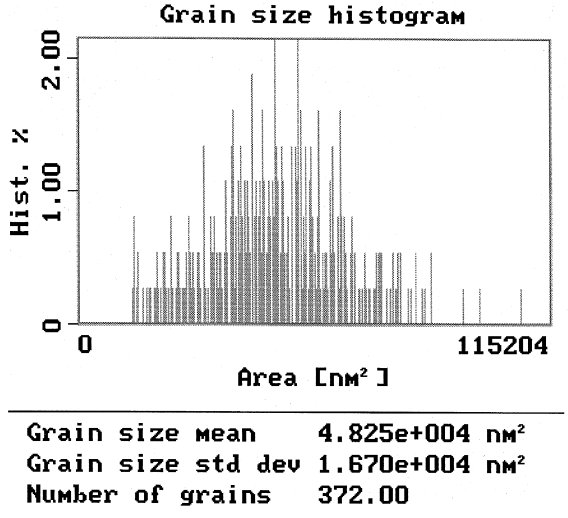

Fig. 5. Histogram of device island size from grain analysis of region B (excluding the oxide regions).

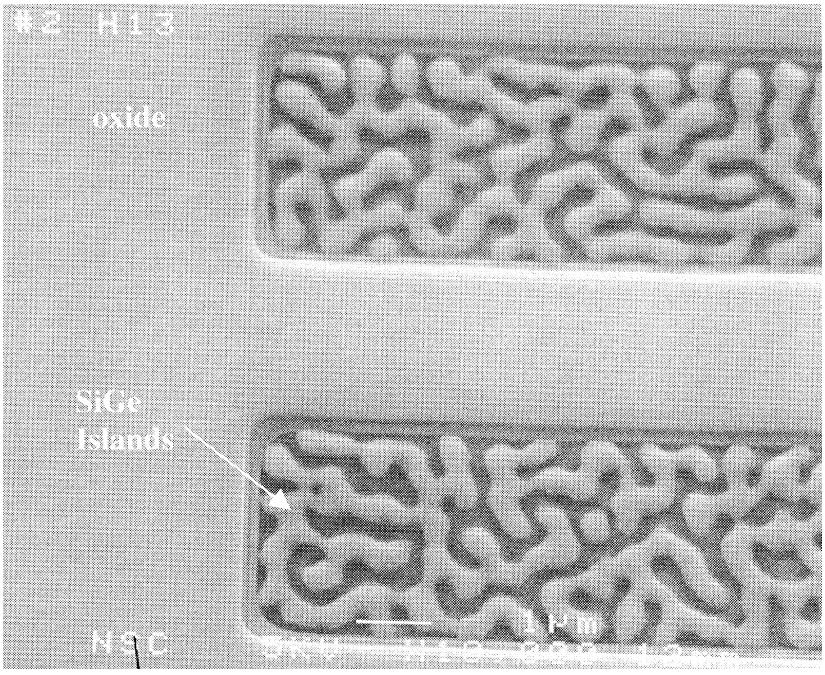

Fig. 6. Angled scanning electron microscope picture of region C of wafer 2 after the thermal annealing subsequent to the growth. Anneal was performed at 750°C for 6 min at 40 Torr in hydrogen.

1.17 nm. This indicates that the initiation of island formation is certainly thermally driven and a lower temperature (with even a longer time as compared to wafer #2) did not form islands to the same extent as the ones at 750°C for 6 min at 40 T. It can also be postulated that the formation of these islands is related to the lateral diffusion of the atoms to adjacent sites. The diffusion of the atoms is related to their mean free path, which is known to be a function of pressure. Hence, an anneal was performed on

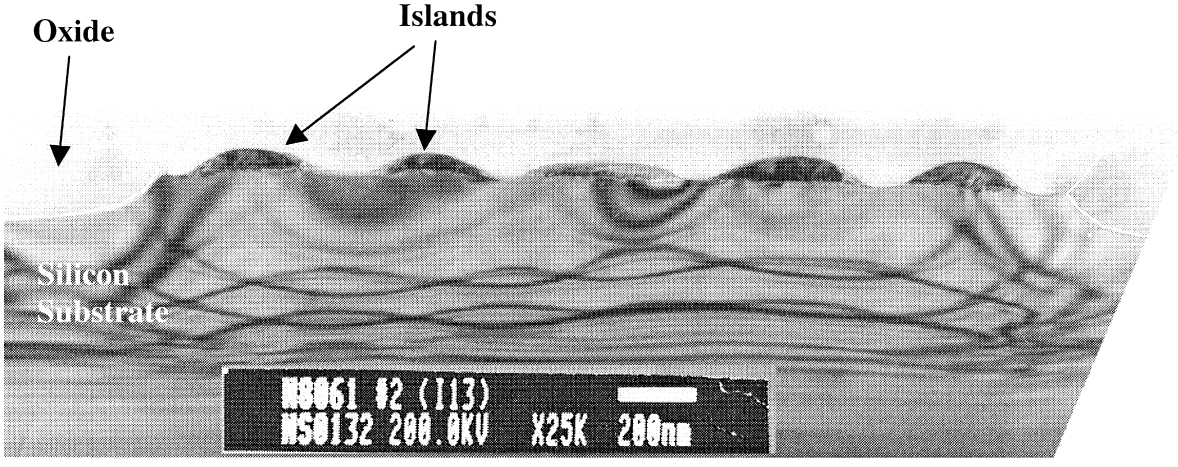

Fig. 7. Cross-sectional TEM of wafer # 1 through region C showing the islands. The oxide edges have been highlighted.

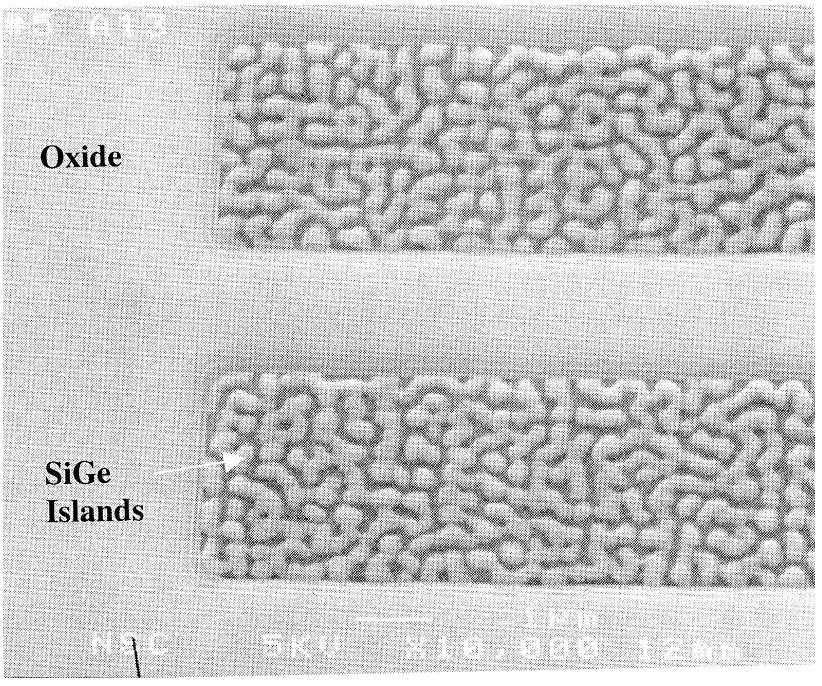

Fig. 8. Angled scanning electron microscope picture region C of wafer 3 after the thermal annealing (subsequent to the growth). Anneal was performed at 650°C for 25 min at 20 Torr in hydrogen.

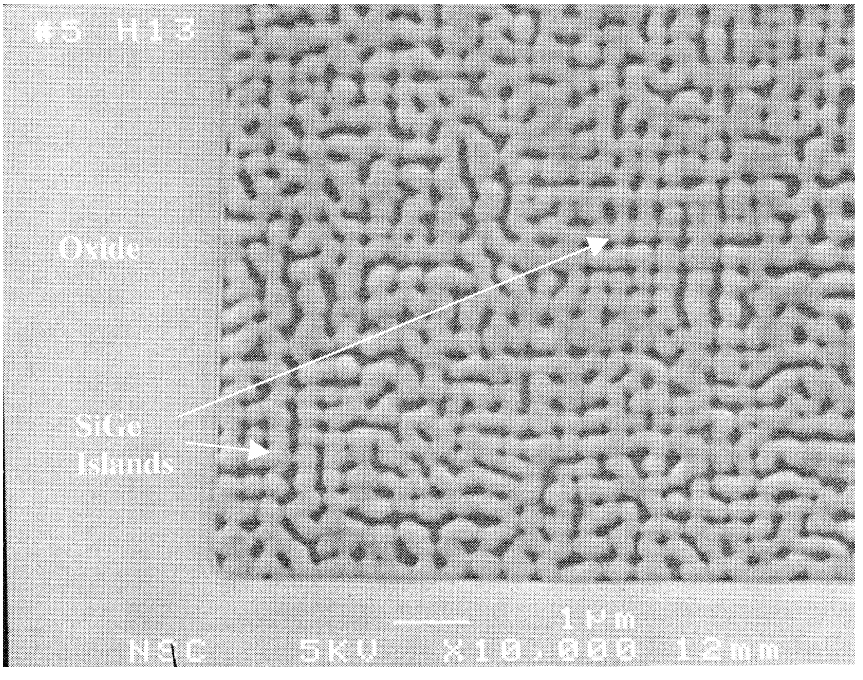

Fig. 9. Angled scanning electron microscope picture in region A of wafer 3 after the thermal annealing (subsequent to the growth). Anneal was performed at 650°C for 25 min at 20 Torr in hydrogen. The islands clearly show order and regularity.

another wafer (#4) at 650°C for 25 min in hydrogen at 20 T to examine the effect on island shape and form. Figs. 8 and 9 show scanning electron microscope image of wafer #4 at location C and A, respectively. As clearly evident from the scanning electron microscope results, the island density, shape, and size is different than the sample annealed at the previous condition. The island size in Fig. 8 is smaller than the ones shown in Fig. 6, which confirms reduced lateral diffusion of the atoms with lower pressure. The islands are still connected to each other as in Fig. 6 and no order is apparent. Clearly the anneal condition parameters such as pressure play a very important role in governing the metastable film relaxation. Wafer #4 in Fig. 9 (region A) shows the most ordered arrangement of sub-micron sized islands when the anneal is performed at 650°C at 20 T for 25 min in hydrogen. When Fig. 9 is compared to Fig. 2, the islands in Fig. 9 are smaller, have a higher density, and are ordered. The grain size analysis was not performed since the islands are not isolated and are still connected. The RMS roughness of islands in Fig. 9 (region A) was found to be 19.8 nm, and the island density was increased to about 11 μm^{-2} clearly indicating an increased packing. From the roughness scans, the maximum height of the islands was found to be 142 nm. The connection between the islands can possibly be removed either by an etching step or by a sacrificial oxidation step. It can also be conjectured that given the proper thickness of the film and anneal conditions, the islands can be made perfectly ordered.

The mechanisms behind the formation of these islands are not clear. However, it can be postulated that the initiation of the island formation is due to the relaxation of the metastable grown film once thermal energy is provided to the system. The mechanisms could be similar in nature to ones governing the SK growth processes. The grown film is strained and in the metastable regime, and hence has not relaxed yet. When thermal energy is provided to the system, the film relaxes and the surface drives to attain the lowest energy, i.e., the islands. A modified form of Ostwald Ripening [7,10,11] could be taking place which assists in the formation of the islands. The initiation can take place from kink sites either at the edges of the oxide/SiGe or from sites of imperfection at the SiGe/Si interface. Lower temperature reduces the formation of the islands. In addition, lateral diffusion of atoms is strongly coupled to the formation of the islands since reducing the pressure reduces the mean free path of the atoms and enhances the formation of the islands.

4. Conclusions

We have demonstrated a technique to form ordered self-assembled device islands using annealing of thin selectively grown SiGe films. The movement and coalescence of the Ge and silicon atoms into islands is determined by their energy and mean free path, which is a function of the ambient conditions, i.e., pressure and temperature. Using the approach presented in this paper, ordered self-assembled device islands can be formed with proper optimization of the anneal conditions. Further detailed experiments need to be performed to understand the nature of the island formation mechanisms as function of initial film thickness and anneal conditions such as pressure, anneal time and gas flows.

References

[1] A. Madhukar, Q. Xie, P. Chen, A. Konkar, Appl. Phys. Lett. 64 (20) (1994) 2727.
[2] N.P. Kobayashi, T.R. Ramachandran, P. Chen, A. Madhukar, Appl. Phys. Lett. 68 (23) (1996) 3299.
[3] J.M. Moison, F. Houzay, F. Barthe, L. Leprince, Appl. Phys. Lett. 64 (2) (1994) 197.
[4] B.R. Bennet, R. Magno, B.V. Shanabrook, Appl. Phys. Lett. 68 (4) (1996) 505.
[5] Y. Peng, B. Wang, W. Chen, S. Liu, Opt. Quantum Electron. 29 (1997) 985.
[6] P. Schittenhelp, M. Gail, J. Brunner, J.F. Nutzel, G. Abstreiter, Appl. Phys. Lett. 67 (9) (1995) 1293.
[7] T.I. Kamins, E.C. Carr, R.S. Williams, S.J. Rosner, J. Appl. Phys. 81 (1) (1997) 211.
[8] T.I. Kamins, R.S. Williams, Appl. Phys. Lett. 71 (9) (1997) 1201.
[9] T.I. Kamins, R.S. Williams, Surf. Sci. 405 (1998) 580–586.
[10] J. Moller, K.I. Jacob, J. Schmelzer, J. Phys. Chem. Solids 59 (6–7) (1998) 1097.
[11] G. Rosenfeld, K. Morgenstern, I. Beckmann, W. Wulfhekel, E. Laegsgaard, F. Besenbacher, G. Comsa, Surf. Sci. 402–404 (1–3) (1998) 401.
[12] T.I. Kamins, D.A.A. Ohlberg, R. Stanley Williams, W. Zhang, S.Y. Chou, Appl. Phys. Lett. 74 (12) (1999) 1773.